JOURNAL OF CATALYSIS 90, 205–220 (1984)

Effects of Metal–Support Interactions on the Hydrogenation of CO over Pd/SiO_2 and Pd/La_2O_3

ROBERT F. HICKS[1] AND ALEXIS T. BELL

Materials and Molecular Research Division, Lawrence Berkeley Laboratory, and Department of Chemical Engineering, University of California, Berkeley, California 94720

Received March 19, 1984; revised June 5, 1984

A study of CO hydrogenation over Pd/SiO_2 and Pd/La_2O_3 has been carried out for the purpose of identifying the effects of Pd dispersion, Pd morphology, and support composition on the catalytic activity of supported Pd. The specific activity of each catalyst for methanol and methane synthesis was determined from microreactor studies carried out at a fixed set of reaction conditions. Palladium dispersion was measured by H_2–O_2 titration, and the morphology of the Pd crystallites, as expressed by the distribution of Pd(100) and Pd(111) planes, was determined from *in situ* infrared spectra of adsorbed CO. The crystallite morphology of the Pd/SiO_2 catalysts is the same, independent of Pd weight loading: 90% of the surface is comprised of Pd(100) planes and 10% of the surface is comprised of Pd(111) planes. By contrast, the crystallite morphology of the Pd/La_2O_3 catalysts changes with Pd loading. Primarily Pd(100) planes are exposed at low-weight loadings while Pd(111) planes are exposed at high-weight loadings. The Pd dispersion has little effect on the methanol turnover frequency over both Pd/SiO_2 and Pd/La_2O_3, for dispersions between 10 and 20%. On the other hand, the methane turnover frequency is independent of Pd dispersion over Pd/SiO_2, but increases with decreasing dispersion over Pd/La_2O_3. It is further observed that the Pd morphology influences the specific activity of Pd/La_2O_3 for methanol synthesis: Pd(100) is nearly threefold more active than Pd(111). For a fixed morphology, the specific methanol synthesis activity of Pd/La_2O_3 is a factor of 7.5 greater than that of Pd/SiO_2.

INTRODUCTION

Poutsma *et al.* (*1*) first demonstrated that supported Pd/SiO_2 catalyzes the synthesis of methanol from CO and H_2. Subsequent work by a number of investigators (*2–12*) has shown that the catalytic properties of Pd for CO hydrogenation are quite sensitive to the composition of the support and the presence of promoters. High activity and selectivity for methanol synthesis are achieved when Pd is supported on rare earth oxides, such as La_2O_3, whereas methane synthesis is preferred when Pd is supported on Group IVB metal oxides, such as TiO_2. For a given support composition, other factors may affect the activity and selectivity of Pd for CO hydrogenation. Thus, Fajula *et al.* (*4*) observed a 20-fold variation in the specific activity for CO hydrogenation and a nearly 100% variation in the selectivity toward methanol depending on the source and grade of silica used. These authors concluded that methanol synthesis is favored on small metal crystallites, while methane formation is enhanced when acidic silicas are used. Boudart and McDonald (*13*) have recently reported that 10-Å particles of Pd are an order of magnitude more active than 180-Å particles for methane synthesis. The large particles also exhibited greater selectivity to methanol at higher pressures. However, Wang *et al.* (*6*) have found that the methanation activity of Pd/Al_2O_3 is independent of Pd crystallite size for particles between 30 and 300 Å in diameter. This led these authors to conclude that for methane synthesis crystallite size is much less important than the composition of the support.

[1] Present address: Research Division, W. R. Grace & Co., 7379 Route 32, Columbia, Maryland 21044.

0021-9517/84 $3.00

Promoters can also have a profound effect on the activity and selectivity of Pd for CO hydrogenation. Driessen *et al.* (*10*) found that promotion of a Pd/SiO_2 catalyst with MgO or La_2O_3 increases the rate of methanol formation. The observation of a parallel increase in the amount of ionic Pd extractable by acetylacetonate led them to conclude that Pd^{n+} ions are required for methanol synthesis. Kikuzono *et al.* (*11*) reported that alkali metal promoters, such as Na_2O, also increase the activity and selectivity of Pd/SiO_2 for methanol synthesis. These authors proposed that the role of the alkali metal is to stabilize a formate species on the Pd surface, which is then easily hydrogenated to produce methanol.

We have studied the properties of Pd/SiO_2 and Pd/La_2O_3 in detail, in order to elucidate the role of the support in promoting methanol synthesis over Pd (*14–16*). Characterization of a series of Pd/SiO_2 and Pd/La_2O_3 catalysts by X-ray photoelectron spectroscopy (XPS) (*14*) and by CO chemisorption (*15*) has revealed the existence of a well-defined metal–support interaction for Pd/La_2O_3. This interaction can be explained by the migration of patches of partially reduced lanthanum oxide onto the Pd particles during sample preparation. These patches are electronegative and transfer charge to the surrounding Pd surface. The charge transfer to Pd is evidenced by a shift in the Pd $3d_{5/2}$ binding energy of Pd/La_2O_3 below that of metallic Pd. Carbon monoxide chemisorption is affected in two ways by the patches of support: CO adsorption is blocked onto the Pd atoms beneath the patches, and, by virtue of the charge transfer, the strength of CO adsorption is weakened on the Pd atoms which surround the patches. By contrast, the XPS spectrum and CO chemisorption characteristics of Pd/SiO_2 show no evidence for an interaction between Pd and the silica support.

This paper reports on a study of CO hydrogenation over a series of Pd/SiO_2 and Pd/La_2O_3 catalysts. The objectives were to differentiate the effects of Pd dispersion and crystallite morphology from the effects of metal–support interactions. Changes in the metal dispersion and morphology with time under reaction conditions were determined from *in situ* infrared spectra of adsorbed CO. All of the observations reported here were for a fixed set of reaction conditions. The influence of reaction conditions on the kinetics of methanol and methane formation over Pd/SiO_2 and Pd/La_2O_3 will be presented separately (*17*).

EXPERIMENTAL

The catalysts used in this study are the same as those used in the XPS and chemisorption studies reported earlier (*14, 15*). The Pd/SiO_2 samples were prepared by incipient wetness impregnation of Cab-O-Sil HS5 silica (BET surface area = 300 m^2/g) with H_2PdCl_4. The Pd/La_2O_3 samples were prepared by ion exchange of fully hydrated La_2O_3 (BET surface area $\simeq$ 11 m^2/g) with H_2PdCl_4. All samples were dried in a vacuum oven at 338 K, calcined in a 21% O_2/He mixture for 2 hr at 623 K, and reduced in H_2 for 3 hr at 523 K. After reduction, the samples were stored in a desiccator.

The concentration of exposed Pd atoms was determined by H_2–O_2 titration, using the pulsed-flow technique (*5*), and the Pd weight loading was determined by X-ray fluorescence and quantitative analysis. Table 1 lists the Pd weight loading, Pd dispersion, D_{Pd}, and the concentration of exposed Pd atoms, C_{Pd_s}, for each of the freshly reduced catalyst samples.

The catalyst activity was determined using a copper microreactor, 4.6 mm i.d. and 3.8 cm long, immersed in a fluidized-bed heater. The amount of catalyst placed in the reactor was 0.1 g. Reaction products were analyzed by gas chromatography using a balanced pair of stainless-steel columns packed with Chromosorb 107. During an analysis, the columns were heated from 313 to 473 K at a rate of 15 K/min. The detection limit of reaction products, determined with a flame ionization detector, was approximately 0.2 ppm.

Investigations of each catalyst sample were initiated by reducing the catalyst in 10 atm of flowing H_2 at 573 K for 3 hr. Synthesis gas with an H_2/CO ratio of 2.5 was then introduced, and the reaction was allowed to proceed at 10 atm and 523 K for 8 to 20 hr. During an experiment, the conversion of CO to methanol, the primary product, was kept below 0.1% of that obtainable at equilibrium.

The infrared spectrum of adsorbed CO was recorded during methanol synthesis in a stainless-steel infrared cell (*18*). Two of these cells were operated in series. A support pellet was suspended in the upstream reactor and a catalyst pellet, of about the same weight, was suspended in the downstream reactor. During an experiment, infrared spectra of the catalyst and the support were collected in quick succession. Later, the support absorbance spectrum was subtracted from the catalyst absorbance spectrum to remove the gas-phase interference from the bands due to chemisorbed CO. All spectra were collected at 8 cm^{-1} resolution on a Digilab FTS-10M Fourier transform infrared spectrometer, equipped with a narrow-band HgCdTe detector. A satisfactory signal-to-noise ratio was obtained by co-adding 100 interferograms.

RESULTS

Pd/SiO_2

Shown in Fig. 1 is a plot of the specific activity of 2.0% Pd/SiO_2 for methanol, dimethyl ether, and methane synthesis with time on stream. The specific activities, N_i, are calculated by dividing the reaction rates by the value of C_{Pd_s} for the freshly reduced catalyst, given in Table 1. Methanol, dimethyl ether, and methane are the only products detected in significant quantity in the reactor effluent. For the reaction conditions chosen, the selectivity to methanol is greater than 90%. In separate experiments, the residence time of the gas in the reactor was varied, and it was found that dimethyl ether is formed by the secondary decomposition of methanol. Therefore, for the remaining discussion only the intrinsic rate of methanol synthesis will be considered, which is represented by $(N_{CH_3OH} + 2N_{(CH_3)_2O})$.

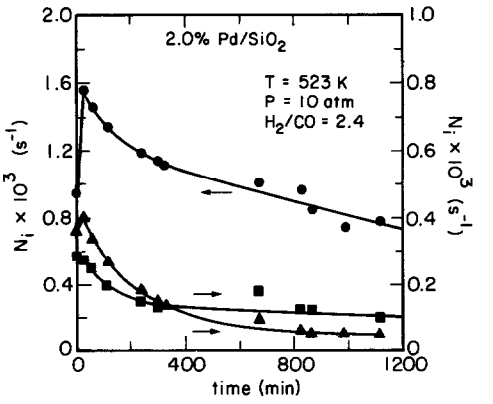

FIG. 1. Dependence of the methanol (●), dimethyl ether (▲), and methane (■) turnover frequencies on reaction time for 2.0% Pd/SiO_2.

A part of the decline in activity with time on stream, seen in Fig. 1, may be ascribed to catalyst sintering. Measurement of the Pd dispersion of 2.0% Pd/SiO_2 after 10 hr of reaction revealed that D_{Pd} had decreased 40% relative to that of the fresh catalyst. As

TABLE 1

Dispersion and Concentration of Exposed Pd Atoms[a]

Catalyst	D_{Pd} (%)	$C_{Pd_s} \times 10^5$ (mol/g)
0.25% Pd/SiO_2	30	0.7
0.75% Pd/SiO_2	28	2.0
2.00% Pd/SiO_2	35	6.5
2.10% Pd/SiO_2	31	6.1
5.10% Pd/SiO_2	26	12.6
9.00% Pd/SiO_2	18	15.3
0.25% Pd/La_2O_3	30	0.7
0.70% Pd/La_2O_3	18	1.2
1.90% Pd/La_2O_3	16	2.9
1.95% Pd/La_2O_3	11	2.1
5.00% Pd/La_2O_3	9	4.1
8.80% Pd/La_2O_3	8	6.9

[a] Determined by H_2–O_2 titration at 298 K on freshly reduced catalyst samples.

TABLE 2

Steady-State Activity of Palladium Catalysts[a]

Catalyst	Turnover frequency ($\times 10^3$ s^{-1})[b]		Selectivity (%) CH_3OH
	CH_3OH	CH_4	
0.25% Pd/SiO_2	1.60	0.06	94.1
0.75% Pd/SIO_2	1.85	0.05	97.5
2.00% Pd/SiO_2	2.15	0.22	92.5
5.10% Pd/SiO_2	2.10	0.24	89.3
9.00% Pd/SiO_2	2.15	0.24	89.1
0.70% Pd/La_2O_3	16.0	0.45	97.4
1.90% Pd/La_2O_3	13.5	0.55	96.5
1.95% Pd/La_2O_3	11.5	0.70	94.3
5.00% Pd/La_2O_3	12.0	1.50	88.7
8.80% Pd/La_2O_3	7.5	1.25	86.1

[a] Reaction conditions: T = 523 K; P = 10 atm; and H_2/CO = 2.5.

[b] Turnover frequencies of Pd/SiO_2 catalysts are corrected for sintering, which occurs during reaction.

will be described below, this level of decrease was confirmed by the observation of a decrease in the integrated intensity of the infrared bands associated with adsorbed CO. The infrared studies also established that the degree of reduction in the dispersion was virtually the same for all of the samples.

Table 2 lists the methanol and methane turnover frequencies and the selectivity to methanol as a function of metal loading for the Pd/SiO_2 catalysts. These values were obtained at reaction times between 8 and 10 hr, and have been corrected to account for catalyst sintering. It is seen that for metal loadings between 2.0 and 9.0% Pd, N_{CH_3OH} and N_{CH_4} are constant. However, for 0.25 and 0.75% Pd/SiO_2, N_{CH_3OH} is slightly lower than that of the other samples, while N_{CH_4} is about a factor of four lower than that of the other samples. In Fig. 2 the turnover frequencies are plotted as a function of the corrected Pd dispersion. With the exception of the points for 0.25% Pd/SiO_2 and 0.75% Pd/SiO_2 (indicated by the open symbols) the data suggest that N_{CH_3OH} and N_{CH_4}

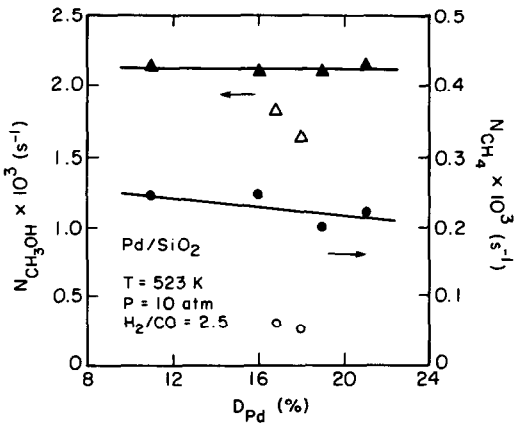

FIG. 2. Correlation of the methanol and methane turnover frequencies with Pd dispersion for the Pd/SiO_2 catalysts.

are independent of Pd dispersion. The inconsistency of the data for the two low-weight loading catalysts is difficult to explain. As will be shown below, the infrared spectra of CO adsorbed on these two catalysts are different in some respects than the spectra observed for the catalysts with Pd weight loadings above 2%.

Infrared spectra of adsorbed CO taken after 1 and 330 min of reaction over the 5.0% Pd/SiO_2 catalyst are shown in Fig. 3. The band at 2070 cm^{-1} is due to linearly bonded CO and those at 1970 and 1920 cm^{-1} are due to bridge-bonded CO (*19, 20*). In subsequent discussions, these three features will be referred to as the L, B_1, and B_2

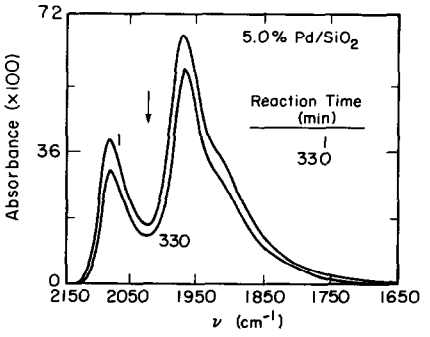

FIG. 3. The infrared spectrum of CO adsorbed on 5.0% Pd/SiO_2 at different times during methanol synthesis. T = 523 K, P = 10 atm, and H_2/CO = 2.4.

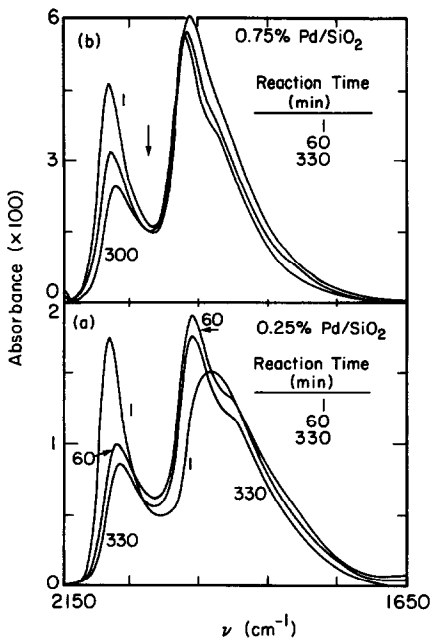

FIG. 4. The infrared spectrum of CO adsorbed on (a) 0.25% Pd/SiO_2 and (b) 0.75% Pd/SiO_2 at different times during methanol synthesis. T = 523 K, P = 10 atm, and H_2/CO = 2.4.

bands, respectively. Figure 3 shows that during the course of the reaction, the positions of the bands do not change, but the intensities of all three bands decrease by about the same degree. The absence of any change in the band positions indicates that the coverage of adsorbed CO does not change with time [see the discussion of frequency shifts given in Ref. (*15*)]. This, in turn, suggests that the reduction in the band intensities is due to a reduction in exposed Pd surface area caused by sintering.

The infrared spectra taken during reaction over the 2.0 and 9.0% Pd/SiO_2 catalysts are virtually the same as shown in Fig. 3. Both samples exhibited a roughly equivalent decrease in the intensity of the bands for linear and bridge-bonded CO. In contrast to these samples, the behavior of the 0.25 and 0.75% Pd/SiO_2 catalysts is different. Figure 4 shows the infrared spectra obtained for these catalysts after 1, 60, and 330 min of reaction. For the 0.25% Pd/SiO_2 sample, the L band is very intense relative to the B_1 and B_2 bands. The latter two bands overlap and their centroid is located near 1940 cm^{-1}. After 60 min under reaction conditions, the L band has diminished greatly in intensity and the B_1 and B_2 bands have become resolved. The appearance of the spectrum at this stage is quite similar to the spectra shown in Fig. 3. When the reaction time is extended to 330 min, the intensity of all the features decreases by about the same extent, much as is seen in Fig. 3. The initial spectrum for the 0.75% Pd/SiO_2 sample also shows a particularly intense L band, but the shape of the overlapping B_1 and B_2 bands is not unusual. With increasing time under reaction conditions, the intensity of the L band decreases rapidly, while that of the B_1 and B_2 bands decreases by only a small amount.

Figure 5 presents a comparison of the infrared spectra observed after 330 min of reaction for five of the Pd/SiO_2 catalysts used in this study. Several characteristic features of each infrared spectrum are listed in Table 3. It is apparent that the five infrared spectra do not differ significantly from one another. The position of the L band lies between 2060 and 2080 cm^{-1}, and that of the B_1 band, between 1955 and 1970 cm^{-1}. The ratio of the maximum absorbance of the L band to that of the B_1 band, A_L/A_{B_1}, lies between 0.45 and 0.60. It is to be noted that neither the positions of the L and B_1 bands, nor the ratio of their maximum intensities, vary in a systematic fashion with metal loading. The only characteristic which does change in such a fashion is the full-width-at-half-maximum of the bridge-bonded bands, $FWHM_B$. This characteristic decreases from 120 to 70 cm^{-1} as the weight loading of Pd increases from 0.25 to 9.0%. Careful examination of Fig. 5 shows that this trend coincides with a decrease in the intensity of the B_2 band, which appears as a shoulder on the low-frequency side of the B_1 band.

The infrared spectra shown in Fig. 5 resemble very closely those reported for CO adsorption at saturation coverage on low-dispersion (≤50%) Pd/SiO_2 catalysts pre-

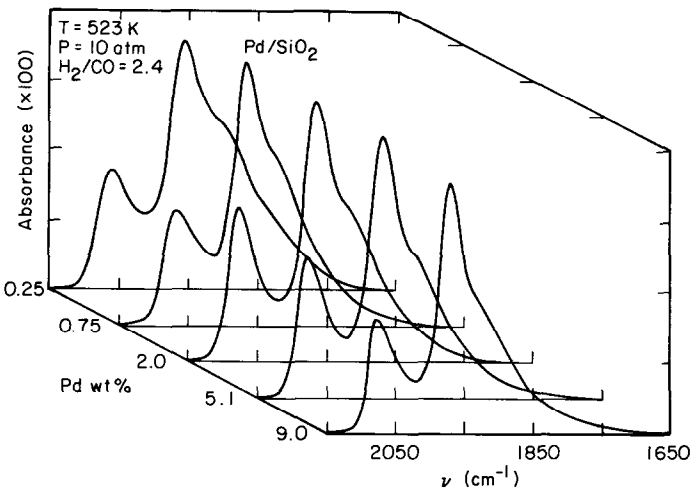

FIG. 5. Infrared spectra of CO adsorbed on the 0.25–9.0% Pd/SiO_2 catalysts at 330 min of reaction.

pared from chloride-containing precursors (*13, 19–21*). Of particular interest is the similarity in the infrared spectrum observed over the 2.0% Pd/SiO_2 catalyst under reaction conditions to that taken for the same catalyst following saturation coverage with CO at 298 K (*15*). For the latter case, the frequencies of the L and B_1 bands, the ratio of the intensities of the L and B_1 bands, and the full-width-at-half-maximum, $FWHM_B$, of the combined B_1 and B_2 bands are ν_L = 2090 cm^{-1}; ν_{B_1} = 1975 cm^{-1}; A_L/A_{B_1} = 0.60; and $FWHM_B$ = 85 cm^{-1}. Each of these characteristics agrees closely with those reported in Table 3 for 2.0% Pd/SiO_2. The coincidence of the infrared spectrum for CO adsorbed under reaction conditions with that for saturation coverage of CO at 298 K strongly suggests that the Pd surface is covered with a monolayer of CO under reaction conditions, i.e., that the ratio of adsorbed CO molecules to the surface Pd atoms under reaction conditions is unity (*15*).

The degree to which sintering occurs during reaction can be estimated from the integrated intensity of the infrared spectrum of adsorbed CO, $\tilde{A}_T$, which is defined by

$$\tilde{A}_T = \frac{\pi R^2 \int_{1600}^{2200} \log_{10}(I_0/I)d\nu}{C_{Pd_S} w_c} \qquad (1)$$

TABLE 3

The Properties of the Infrared Spectrum of Adsorbed CO on Pd/SiO_2 Recorded during Methanol Synthesis[a]

Catalyst	Frequency (cm^{-1})		A_l/A_{B_1}	$FWHM_B$ (cm^{-1})	$\tilde{A}_T \times 10^{-6}$ (cm/mol)
	ν_L	ν_{B_1}			
0.25% Pd/SiO_2	2060	1955	0.50	120	21
0.75% Pd/SiO_2	2070	1970	0.45	90	16
2.00% Pd/SiO_2	2075	1965	0.60	85	21
5.10% Pd/SiO_2	2080	1970	0.55	80	24
9.00% Pd/SiO_2	2075	1970	0.45	70	25

[a] Reported values are based on observations after 330 min of reaction.

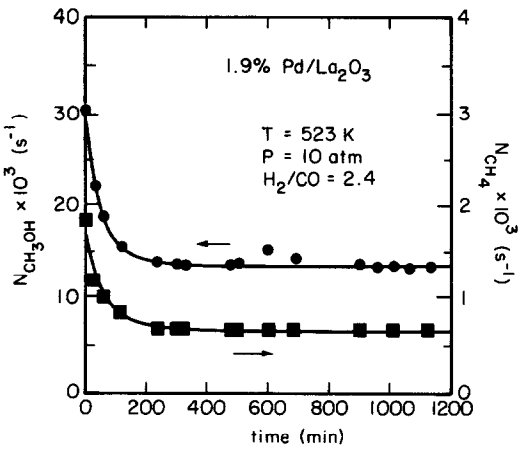

FIG. 6. Dependence of the methanol and methane turnover frequencies on reaction time for 1.9% Pd/La_2O_3.

In Eq. (1), πR^2 is the cross-sectional area of the catalyst disk, $\log_{10}(I_0/I)$ is the absorbance, ν is the frequency, C_{Pd_s} is the concentration of exposed Pd atoms, and w_c is the weight of the catalyst disk. Values of $\tilde{A}_T$ for five of the Pd/SiO_2 samples, obtained after 330 min of reaction, are shown in Table 3. These values were calculated assuming C_{Pd_s} to be equal to that of the freshly reduced catalyst (see Table 1). The decrease in C_{Pd_s} with reaction time is determined by dividing $\tilde{A}_T$ evaluated after 330 min of reaction by the value of $\tilde{A}_T$ for saturation coverage of CO at 298 K. For 2.0% Pd/SiO_2, the latter value of $\tilde{A}_T$ is 36.4×10^6 cm/mol (*15*). From this calculation, it is concluded that C_{Pd_s} decreases from 6.5×10^5 to 3.8×10^5 mol/g, which corresponds to a 42% decrease in the Pd dispersion. This decrease in dispersion is in close agreement with that determined by H_2–O_2 titration for a used 2.0% Pd/SiO_2 sample. As can be seen in Table 3, the magnitude of $\tilde{A}_T$ is about the same for each Pd/SiO_2 catalyst, from which it is concluded that each catalyst sinters to about the same degree.

Pd/La_2O_3

Methanol and methane are the only products formed during the hydrogenation of CO over Pd/La_2O_3. Shown in Fig. 6 is a plot of the specific activity for methanol and methane synthesis of 1.9% Pd/La_2O_3 with time on stream. For this catalyst, the rapid decrease in activity which occurs during the first hour of reaction is not related to catalyst sintering. Measurements of Pd dispersion performed on a used sample of 1.9% Pd/La_2O_3 showed little decrease in the initial value of D_{Pd}. With the exception of 0.25% Pd/La_2O_3, the behavior of all of the Pd/La_2O_3 catalysts is similar to that shown for 1.9% Pd/La_2O_3 in Fig. 6. The 0.25% Pd/La_2O_3 catalyst, on the other hand, was found to sinter with time on stream. The behavior of this catalyst is discussed separately at the end of this section.

The specific activities of the Pd/La_2O_3 catalysts for methanol and methane synthesis are listed in Table 2. The turnover frequencies shown in the table were measured after 8 to 10 hr of reaction. Comparison of the data for Pd/La_2O_3 with that for Pd/SiO_2 reveals that for the reaction conditions studied, Pd/La_2O_3 is from 3.5 to 7.5 times more active for methanol synthesis. The dependencies of N_{CH_3OH} and N_{CH_4} on Pd dispersion for Pd/La_2O_3 are shown in Fig. 7. It is observed that N_{CH_3OH} increases, while N_{CH_4} decreases, as the Pd dispersion increases from 8 to 18%. This is in strong contrast to the results for Pd/SiO_2, which

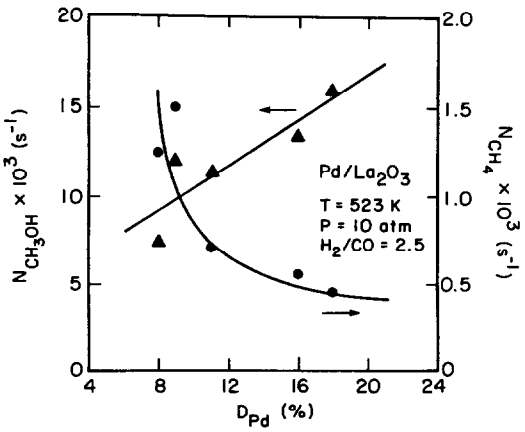

FIG. 7. Correlation of the methanol and methane turnover frequencies with Pd dispersion for the 0.7–8.8% Pd/La_2O_3 catalysts.

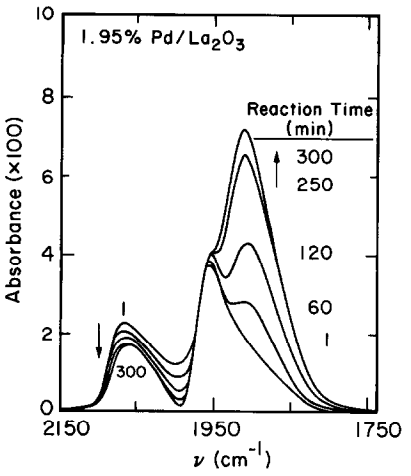

FIG. 8. The infrared spectrum of CO adsorbed on 1.95% Pd/La_2O_3 at different times during methanol synthesis. T = 523 K, P = 10 atm, and H_2/CO = 2.4.

evidence no change in the methanol and methane turnover frequencies with D_{Pd} over a similar range of dispersions.

A series of infrared spectra for CO adsorbed on 1.95% Pd/La_2O_3 taken under reaction conditions is shown in Fig. 8. The positions of the L, B_1, and B_2 bands are 2050, 1955, and 1900 cm^{-1}, respectively. The change in the infrared spectrum with reaction time, depicted in Fig. 8, is quite unusual. For the first 30 min of reaction, only the L and B_1 bands are observed, and the infrared spectrum is virtually identical to that for saturation coverage of CO on 1.95% Pd/La_2O_3 at 298 K (*15*). As the reaction proceeds, the B_2 band grows in intensity, while the L band declines in intensity. The intensity of the B_1 band, however, does not change. It is also noted that the positions of all three bands remain essentially the same during the entire 300 min of reaction.

The infrared spectrum of CO adsorbed on 0.7, 1.9, 5.9, and 8.8% Pd/La_2O_3 changed with time in a manner very similar to that shown in Fig. 8 for 1.95% Pd/La_2O_3. However, the spectrum observed after 330 min of reaction was strongly characteristic of the Pd weight loading. Figure 9 shows that while the positions of the L, B_1, and B_2 bands do not depend on weight loading, the distribution of band intensities does. As the Pd weight loading increases, the B_1 band becomes less intense relative to the B_2 band, and the fraction of the total integrated absorbance associated with the L band decreases. A number of characteristics for each of the spectra presented in Fig. 9 are listed in Table 4.

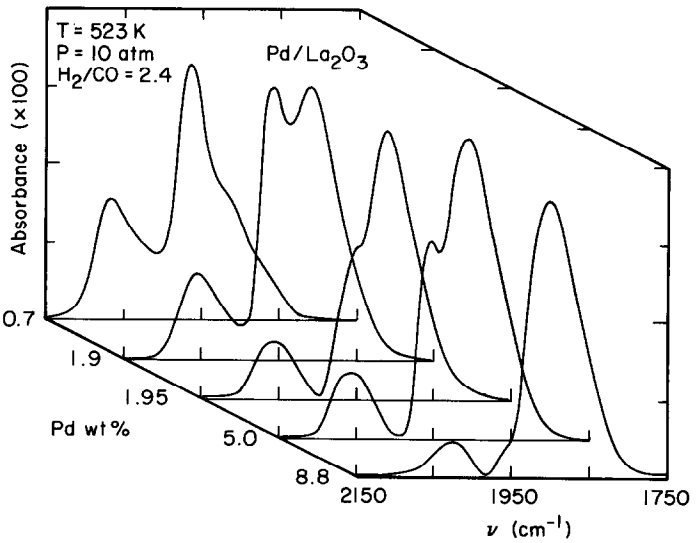

FIG. 9. Infrared spectra of CO adsorbed on the 0.7–8.8% Pd/La_2O_3 catalysts at 330 min of reaction.

TABLE 4

The Properties of the Infrared Spectrum of Adsorbed CO on Pd/La_2O_3 Recorded during Methanol Synthesis[a]

Catalyst	Frequency (cm^{-1})			A_1/A_{B_1}	$FWHM_B$ (cm^{-1})	$\bar{A}_T \times 10^{-6}$ (cm/mol)
	ν_L	ν_{B_1}	ν_{B_2}			
0.25% Pd/La_2O_3	2060	1960	1900	0.65	80	3.3[b]
0.70% Pd/La_2O_3	2060	1965	1900	0.45	65	10.6
1.90% Pd/La_2O_3	2060	1955	1900	0.35	115	10.4
1.95% Pd/La_2O_3	2050	1955	1900	0.45	110	8.4
5.00% Pd/La_2O_3	2060	1955	1900	0.40	110	10.4
8.80% Pd/La_2O_3	2040	1955	1900	—	75	—

[a] Reported values are for observations after 330 min of reaction.
[b] Low value of $\bar{A}_T$ caused by sintering.

The fraction of CO adsorbed on B_2 sites after 330 min of reaction, X_{B_2}, can be determined from the expression

$$X_{B_2} = \frac{\tilde{A}_B(330) - \tilde{A}_B(1)}{\tilde{A}_B(330)}, \qquad (2)$$

where $\tilde{A}_B(1)$ and $\tilde{A}_B(330)$ are the integrated absorbances for the overlapping B_1 and B_2 bands in the region between 2000 and 1750 cm^{-1} at reaction times of 1 and 330 min, respectively. An implicit assumption in Eq. (2) is that the extinction coefficients for the B_1 and B_2 bands are equivalent. The fraction of CO adsorbed on B_1 sites is then given by

$$X_{B_1} = 1 - X_{B_2}. \qquad (3)$$

Values of X_{B_1} for each of the Pd/La_2O_3 catalysts are listed in Table 4 and are plotted versus D_{Pd} in Fig. 10. It is observed that X_{B_1} increases from 0.1 to 0.85 as the Pd weight loading decreases, and, hence, as the dispersion increases from 8 to 18%.

The total integrated absorbance for adsorbed CO, $\tilde{A}_T$, was calculated for the spectrum recorded at 330 min of reaction using Eq. (1), and the results are listed in Table 4 for four of the Pd/La_2O_3 samples. The values of $\tilde{A}_T$ are virtually the same for each sample, even though the values of X_{B_1} are quite different. This suggests that the integrated absorption coefficient is essentially the same for CO adsorption on B_1 and B_2 sites. The coverage by adsorbed CO can be estimated by dividing $\tilde{A}_T$ by $\bar{A}_T$, the total integrated absorption coefficient. Using a value of $\bar{A}_T = 10.7 \times 10^6$ cm/mol obtained from CO adsorption experiments (*15*), it is determined that the CO coverage of the Pd crystallites after 330 min of reaction is close to unity.

The time-dependent behavior of the infrared spectrum for 0.25% Pd/La_2O_3 is quite different from that for the higher weight loading samples. A series of infrared spec-

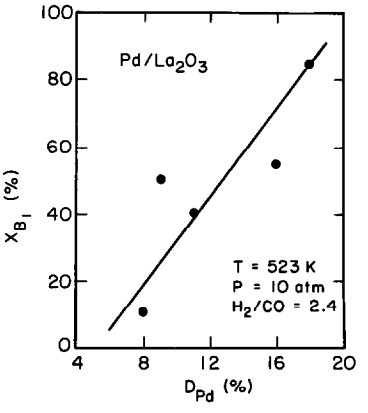

FIG. 10. Correlation of the fraction of bridge-bonded CO that is adsorbed on B_1 sites with Pd dispersion for 0.7–8.8% Pd/La_2O_3.

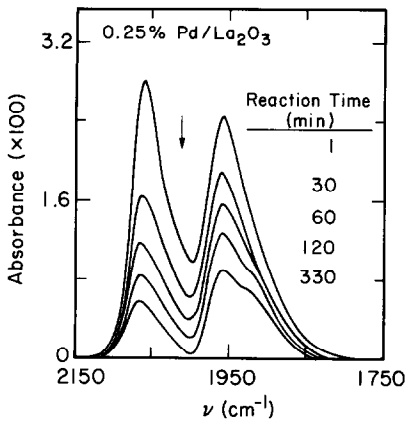

FIG. 11. The infrared spectrum of CO adsorbed on 0.25% Pd/La_2O_3 at different times during methanol synthesis. T = 523 K, P = 10 atm, and H_2/CO = 2.4.

tra collected during 330 min of reaction over 0.25% Pd/La_2O_3 is shown in Fig. 11. The spectrum after 1 min of reaction exhibits an intense L band and a well-defined B_1 band, but no evidence for a B_2 band. The magnitude of the total integrated absorbance is 12.5×10^6 cm/mol. Since this value of $\tilde{A}_T$ is close to that for saturation coverage, 10.7×10^6 cm/mol, it is concluded that surface of the Pd crystallites is completed saturated by CO after 1 min of reaction. With time the intensity of the L and B_1 bands diminishes and a B_2 band begins to appear. The absence of a change in the positions of the L and B_1 band indicates that the reduction in band intensity can be ascribed to a loss in Pd surface area due to sintering of the Pd microcrystallites.

The effect of catalyst sintering on the dispersion and specific activity of 0.25% Pd/La_2O_3 was taken into account through the use of Eqs. (4) and (5).

$$D_{Pd}(t) = D_{Pd}(0)\frac{\tilde{A}_T(t)}{\tilde{A}_T(0)} \quad (4)$$

$$N_i'(t) = N_i(t)\frac{\tilde{A}_T(0)}{\tilde{A}_T(t)}. \quad (5)$$

Here, $D_{Pd}(0)$ is the initial dispersion, $\tilde{A}_T(t)$ and $\tilde{A}_T(0)$ are the total integrated absorbances of the infrared spectrum at times t and zero, and $N_i(t)$ is the turnover frequency of species i at time t based on the initial dispersion, $D_{Pd}(0)$. Shown in Fig. 12 is a plot of N'_{CH_3OH} and N'_{CH_4} versus $D_{Pd}(t)$ for 0.25% Pd/La_2O_3. The methanol turnover frequency decreases by about 20% over a fourfold decrease in Pd dispersion. This degree of change is considerably less than that observed in Fig. 7. The methane turnover frequency, on the other hand, increases threefold as the Pd dispersion decreases from 30 to 7%. This latter correlation is in qualitative agreement with the dependence of N_{CH_4} on D_{Pd} seen in Fig. 7.

DISCUSSION

The results presented in Table 2 clearly illustrate that for a fixed set of reaction conditions, the specific rates of methanol and methane synthesis can be a factor of five or more higher for Pd/La_2O_3 than for Pd/SiO_2. Figures 2, 7, and 12 show that the extent to which Pd dispersion influences the specific activities for methanol and methane synthesis strongly depends on the support composition and the manner in which the change in Pd dispersion is effected. Since significant insights into individual influences of dispersion, weight loading, and support composition can be obtained from an inter-

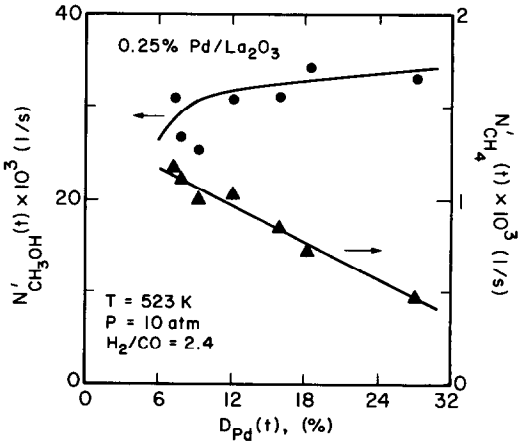

FIG. 12. Correlation of the methanol and methane turnover frequencies with the instantaneous Pd dispersion for 0.25% Pd/La_2O_3.

pretation of the infrared spectra of adsorbed CO, it is useful to discuss these data first.

Infrared Observations of CO Hydrogenation

The B_1 and B_2 bands observed in the spectra taken under reaction conditions are similar to those reported by numerous authors for CO adsorption on supported Pd catalysts (*15, 21–24*). It has been proposed (*24–27*) that these features can be assigned to CO adsorption on Pd(100) and Pd(111) surfaces, based on the close agreement of the frequencies of the B_1 and B_2 bands with those for CO adsorption on Pd single-crystal surfaces, reported by Bradshaw and Hoffmann (*26–28*). Combined LEED and infrared observations indicate that on the Pd(100) surface, CO is adsorbed onto twofold bridging sites for CO coverages between 0.006 and 0.82. On the Pd(111) surface adsorbed CO can occupy both twofold and threefold sites. Adsorption onto threefold sites occurs for CO coverages of 0.009 to 0.3. Above a coverage of 0.3, the adlayer is compressed so that twofold sites are occupied.

The L band observed under reaction conditions resembles that seen in previous studies with both supported and unsupported Pd (*15, 19–23, 29–33*). This feature is attributed to linearly adsorbed CO. While Bradshaw and Hoffmann (*26, 27*) note that linearly adsorbed CO can occur on Pd(100) and Pd(111) surfaces, studies by other authors (*21, 29–32*) suggest that adsorption in a linear form can occur on Pd atoms located at the corners and edges of intersecting crystal planes, and at other low-coordination sites. Such sites are expected to be present in high concentration when the surfaces of the Pd crystallites are rough, or when the size of the crystallites is small.

The preceding discussion suggests that the infrared spectrum of CO adsorbed on supported Pd can provide information regarding the morphology of supported Pd crystallites. The distribution between the low-index Pd(100 and Pd(111) planes is obtained from the relative intensities of the B_1 and B_2 bands. On the other hand, the relative intensity of the L band provides information about the size and roughness of the crystallites. With these ideas in mind, we consider next the spectra observed under reaction conditions for Pd/SiO_2 and Pd/La_2O_3.

The infrared spectra for 0.25 and 0.75% Pd/SiO_2, presented in Fig. 4, indicate that at the start of reaction, the intensity of the L band is comparable to that of the B_1 band. This is in contrast to the relative intensities of the bands seen in the infrared spectrum for 5.0% Pd/SiO_2, shown in Fig. 3. Since the initial dispersions for all three catalysts are similar, the observed differences in the ratio of L and B_1 band intensities is attributed to a greater roughness of the Pd crystallites in the 0.25 and 0.75% Pd/SiO_2 samples than in the 5.0% Pd/SiO_2 sample. This interpretation agrees with the observations of Bradshaw and Hoffmann (*33*) for CO adsorption on polycrystalline Pd foil. These authors observed a strong L band when CO was adsorbed on an unannealed foil. With progressive annealing, the intensity of the L band decreased relative to that of the B_1 and B_2 bands. It was proposed that annealing causes a reduction in the number of edge, kink, and defect sites. The reason why the surfaces of the Pd crystallites in the two low-weight loading catalysts are rougher than the surfaces of the Pd crystallites in the 5.0% Pd/SiO_2 catalyst is difficult to identify. One possibility is that it is due to the amount of chlorine present in the gas phase during calcination. For the same mass of catalyst, the chlorine partial pressure will be lower, the lower the metal loading. Since chlorine is known to assist the redistribution of Group VIII metals (*34*), high partial pressures of chlorine could be expected to accelerate the annealing of defects at the surfaces of the Pd crystallites. It is interesting to note in this context that van Hardeveld and Hartog (*22*) have observed that spectra of CO adsorbed on Pd/SiO_2 cat-

alysts prepared from palladium acetate exhibit a much more intense L band than the spectra for CO adsorbed on Pd/SiO_2 catalysts prepared from palladium chloride.

The changes with time observed in the infrared spectra of the low weight loading catalysts suggest that the Pd crystallites in these samples are annealed during exposure to reaction conditions. Thus, after 330 min of reaction the spectra of all the catalysts are remarkably similar, as can be seen in Fig. 5. It is to be noted that the ratio of the absorbance intensities of the L and B_1 bands for these five spectra does not change significantly even though the Pd dispersion varies from 11 to 21%. The relative intensity of the L band is not affected much by Pd dispersion presumably because the crystallites are large (between 100 and 200 Å) and contain a relatively low concentration of low-coordination sites. The much greater intensity of the B_1 band relative to the B_2 band further signifies that the surfaces of the Pd crystallites supported on silica consist predominately of Pd(100) planes.

The time-dependent behavior of the infrared spectra for the Pd/La_2O_3 catalysts with weight loadings above the 0.25% Pd differs from that for the Pd/SiO_2 catalysts. As shown in Fig. 8 for 1.95% Pd/La_2O_3, the intensity of the L and B_1 bands remain fairly constant with time under reaction conditions, indicating that no sintering occurs. What is observed, though, is a progressive increase in the intensity of the B_2 band. This peculiar behavior can be understood, if one considers the metal–support interaction which occurs between Pd and La_2O_3. As noted earlier, characterization of Pd/La_2O_3 by XPS (*14*) and by H_2 and CO chemisorption (*15*) have suggested that patches of partially reduced support are deposited on the Pd particles during sample preparation. Infrared observations of CO chemisorption at 298 K (*15*) indicate that CO adsorbs to full coverage on only part of the Pd surface, and that this surface is comprised exclusively of Pd(100) planes. Based on this evidence, we conclude that the patches selectively cover the Pd(111) planes of a freshly reduced catalyst. The similarity of the spectra observed for CO adsorption at 298 K and for the first 30 min of reaction indicates that the structure of the catalyst is the same in both cases. The gradual appearance of the B_2 band, seen in Fig. 8, suggests that with increasing time under reaction conditions the interaction between the patches of the partially reduced support and the Pd(111) surfaces is altered in such a fashion that CO adsorption on these planes can now occur. What causes the metal–support interaction to be weakened during reaction is unclear. Possibly, water formed from the methanation reaction reacts with the patches and breaks down the interaction. Thus, for example, Duprez and Miloudi (*35*) have reported that strong metal–support interactions between Group VIII transition metals and TiO_2 can be destroyed by water exposure at elevated temperatures.

The XPS and chemisorption studies (*14, 15*) have further shown that the patches of partially reduced support cover a greater percentage of the crystallites on the high-weight loading–low-dispersion catalysts. Thus, for example, the amount of CO which can adsorb on the Pd at 298 K decreases from 0.42 to zero as the Pd dispersion decreases from 18 to 8%. This correlation is also evidenced by the present results. The fraction of the Pd surface that can adsorb CO during the first 30 min of reaction is given by X_{B_1}, and as shown in Fig. 10, X_{B_1} decreases from 0.85 to 0.10 as the Pd dispersion decreases from 18 to 8%. Since the patches of partially reduced support affect the morphology of the Pd crystallites, it is possible to control the morphology by controlling the extent of the metal–support interaction. Preparation of low-weight loading–high-dispersion catalysts favors Pd(100) surfaces, while preparation of high-weight loading–low-dispersion catalysts favors Pd(111) surfaces.

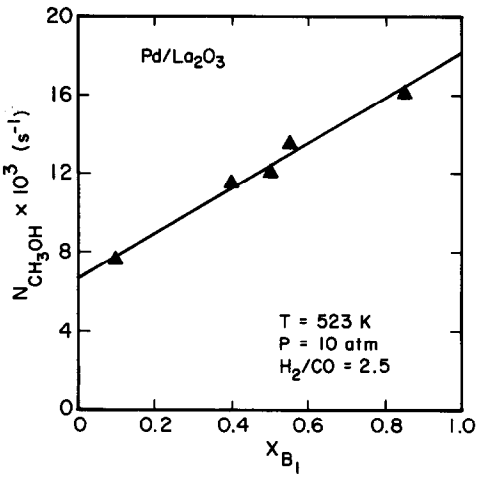

FIG. 13. Correlation of the methanol turnover frequency with the fraction of bridge-bonded CO that is adsorbed on B_1 sites for Pd/La_2O_3.

Activity of Pd Catalysts for CO Hydrogenation

The data in Fig. 2 indicate that the specific activity of Pd/SiO_2 for methanol synthesis is independent of the Pd dispersion for dispersions between 10 and 20%. For these dispersions, metal particle diameters are estimated to be between 100 and 200 Å. It should be noted that the Pd morphology does not change with the dispersion of these catalysts, and so the effect of this variable on the synthesis of methanol over Pd/SiO_2 cannot be considered.

For Pd/La_2O_3, the dependence of the methanol turnover frequency on the Pd dispersion depends on whether the dispersion is decreased by increasing the Pd weight loading (Fig. 7), or by sintering a catalyst with a fixed-weight loading (Fig. 12). An explanation of the different behaviors observed in the two figures may be related to an effect of Pd morphology on the intrinsic activity of Pd for methanol synthesis. The catalysts with metal loadings from 0.7 to 8.8% differ in Pd morphology as well as Pd dispersion, and as shown in Fig. 10, the morphology varies with dispersion in a systematic fashion. Thus, low methanol turnover frequencies are observed at low dispersion and high fraction of B_2 adsorption sites, while high methanol turnover frequencies are observed at high dispersion and high fraction of B_1 adsorption sites. On the other hand, when the 0.25% Pd/La_2O_3 catalyst is sintered, the Pd morphology changes little until near the end of the experiment. This behavior is evidenced by the infrared spectra for 0.25% Pd/La_2O_3 shown in Fig. 11. The data in Fig. 12 indicate that the methanol turnover frequency remains nearly constant, if the Pd dispersion is decreased without a change in Pd morphology. In fact, the sudden decline in N_{CH_3OH} observed in Fig. 12 at dispersions near 7% is very likely due to an increase in B_2 adsorption sites relative to B_1 adsorption sites at long reaction times (see Fig. 11). It appears, therefore, that Pd dispersion does not affect the specific activity of Pd/La_2O_3 for methanol synthesis, but that Pd morphology does.

To illustrate the effect of Pd morphology on the methanol synthesis activity of Pd/La_2O_3, N_{CH_3OH} has been plotted versus X_{B_1} in Fig. 13 for the 0.7 to 8.8% Pd/La_2O_3 catalysts. It is seen that the methanol turnover frequency increases linearly with X_{B_1} and that there is very little scatter in the data. Assuming that the infrared assignments discussed earlier are correct, the trend in Fig. 13 suggests that the methanol turnover frequency depends on the orientation of the metal surface: for Pd(100) planes, $N_{CH_3OH} = 18 \times 10^{-3}$ s^{-1}; and for Pd(111) planes, $N_{CH_3OH} = 6.5 \times 10^{-3}$ s^{-1}.

The dependence of the methanol turnover frequency on the orientation of the Pd surface, suggests that methanol synthesis can occur on planar surfaces. This interpretation is further consistent with there being no intrinsic effect of particle size, since if sites of low coordination were unusually active for methanol synthesis, an effect of Pd dispersion on the methanol turnover frequency should have been observed. Recent studies of methanol decomposition on Pd

single crystals (*36, 37*) also support this conclusion. It was reported that at temperatures above 300 K, methanol spontaneously decomposes into CO and H_2 over Pd(100) and Pd(111) single-crystal surfaces. By the principle of microscopic reversibility, methanol synthesis from CO and H_2 should proceed over Pd(100) and Pd(111) under suitable conditions of temperature and pressure.

The preceding discussion demonstrates that in any assessment of the influence of metal–support effects, proper recognition must be given to the effects of crystallite morphology. In the case of the present studies, examination of the spectra in Figs. 5 and 9 indicate that the morphology of the Pd crystallites occurring on the 0.7% Pd/La_2O_3 sample is similar to that of the crystallites on the 5.1% Pd/SiO_2 sample. The specific activity of 0.7% Pd/La_2O_3 is 1.6×10^{-2} s^{-1}, while the specific activity of 5.1% Pd/SiO_2 is 2.1×10^{-3} s^{-1}. Thus, the increase in the methanol turnover frequency of La_2O_3-supported Pd over that of SiO_2-supported Pd, attributable solely to metal–support effects, is 7.5.

The results obtained here do not allow us to explain why for a given Pd crystallite morphology the specific rate of methanol synthesis over Pd/La_2O_3 is higher than that for methanol synthesis over Pd/SiO_2. To address this question, it is necessary to know whether the support composition affects the dependence of N_{CH_3OH} on reactant partial pressures and temperature. The influence of these variables has been investigated and will be reported separately, together with a discussion of the mechanism of methanol synthesis over Pd/SiO_2 and Pd/La_2O_3 (*17*).

The effects of Pd dispersion and morphology on the specific rate of methane synthesis are examined next. For Pd/SiO_2, the data in Fig. 2 show little variation in the methane turnover frequency with Pd dispersion. The only exceptions are the data for 0.25 and 0.75% Pd/SiO_2. The values of N_{CH_4} for these two catalysts are comparable, but a factor of four less than the values of N_{CH_4} for the other four catalysts. No definite reason can be given for this difference, since neither the infrared spectra of adsorbed CO (see Fig. 5) nor the XPS spectra (*14*) for these catalysts are sufficiently different from those of the higher-weight-loading catalysts to provide a clue.

The apparent absence of a dependence of methane turnover frequency on Pd dispersion for Pd/SiO_2, reported here, is in good agreement with the conclusions of Vannice and co-workers (*5, 6*). These authors reported that for both SiO_2- and Al_2O_3-supported Pd, the methane turnover frequency is independent of Pd particle size for particles ranging from 30 to 300 Å. It is interesting to note, though, that Boudart and McDonald (*13*) have recently reported that 10-Å particles are an order of magnitude more active than 180-Å particles for methane synthesis. The high activity of the 10-Å particles was attributed to the special ability of small Pd particles to dissociate CO.

For Pd/La_2O_3, the methane turnover frequency increases with decreasing Pd dispersion, regardless of whether the dispersion is decreased by increasing the Pd weight loading (Fig. 7), or by sintering of the 0.25% Pd/La_2O_3 catalyst (Fig. 12). This dependence is in strong contrast to that observed for methane synthesis over Pd/SiO_2 but is similar to that observed for methane synthesis over Ni and Ru catalysts (*13, 38, 39*). A change in the structure sensitivity of the reaction with support composition suggests that the mechanism of methane synthesis over Pd/SiO_2 and Pd/La_2O_3 may be different. A further discussion of this question and its implications for catalysis by Pd will be presented separately (*17*). It should be noted that since the methane turnover frequency is influenced by Pd dispersion, the effect of Pd morphology on N_{CH_4} cannot be ascertained from the data given in Table 2.

CONCLUSIONS

Changes in the dispersion and morphol-

ogy of SiO_2- and La_2O_3-supported Pd catalysts during CO hydrogenation can be determined from *in situ* infrared spectra of adsorbed CO. Catalysts with Pd weight loadings of 2% or more show no evidence of sintering when La_2O_3 is the support. When supported on SiO_2, Pd sinters by about 40% over a 300-min period under reaction conditions. For Pd loadings of less than 1%, sintering is observed for both SiO_2- and La_2O_3-supported Pd catalysts. The morphology of the Pd crystallite surfaces is assessed from the distribution of integrated intensities of the B_1 and B_2 bands for the two forms of bridge-bonded CO. Based on the similarity in the positions of these bands to those in single crystal studies, it is concluded that the B_1 band characterizes adsorption on Pd(100) surfaces and the B_2 band characterizes adsorption on Pd(111) surfaces. Following exposure to reaction conditions for 330 min, the distribution of B_1 and B_2 band intensities is roughly the same for all of the Pd/SiO_2 catalysts examined, indicating the Pd crystallite are composed of approximately 90% Pd(100) and 10% Pd(111) surfaces. *In situ* infrared observation reveal that CO adsorption onto Pd(111) surfaces of Pd/La_2O_3 catalysts is initially inhibited, but does occur with increasing time under reaction conditions. Under steady-state conditions, the distribution of Pd(100) and Pd(111) surfaces is a strong function of the Pd weight loading. The unusual behavior of Pd/La_2O_3 is attributed to coverage of the Pd(111) surfaces of the freshly reduced catalyst by patches of partially reduced support. Under reaction conditions the interaction between the metal and the patches gradually decreases, allowing CO chemisorption to occur on the Pd(111) surfaces.

For Pd/SiO_2, the methanol and methane turnover frequencies are independent of Pd dispersion, for dispersions between 11 and 21%. For Pd/La_2O_3, the methanol turnover frequency is independent of Pd dispersion, but the methane turnover frequency decreases with increasing Pd dispersion, for dispersions between 8 and 18%. The methanol synthesis activity of Pd/La_2O_3 is also found to depend on the Pd morphology: Pd(100) surfaces exhibit roughly threefold greater activity than Pd(111) surfaces. For an equivalent distribution of Pd(100) and Pd(111) surfaces, the specific activity for methanol synthesis is a factor of 7.5 greater for La_2O_3- than for SiO_2-supported Pd.

APPENDIX: NOMENCLATURE

A_{B_1}	Absorbance maximum of B_1 infrared band
A_L	Absorbance maximum of L infrared band
$\tilde{A}_B$	Integrated absorbance of the infrared spectrum of bridge-bonded CO, cm/mol
$\tilde{A}_T$	Total integrated absorbance of the infrared spectrum of adsorbed CO, defined by Eq. (1), cm/mol
C_{Pd_s}	Concentration of exposed Pd atoms, mol/g of catalyst
D_{Pd}	Pd dispersion
$FWHM_B$	Full-width-at-half-maximum of infrared band for bridge-bonded CO, cm^{-1}
I	Intensity of the infrared spectrum at a given vibrational frequency
N_i	Turnover frequency for product i, s^{-1}
R	Radius of sample disk, cm
w_c	Weight of sample disk, g
X_{B_1}	Fraction of bridge-bonded CO that is B_1
X_{B_2}	Fraction of bridge-bonded CO that is B_2
ν_i	Vibrational frequency of species i, cm^{-1}

ACKNOWLEDGMENT

This work was supported by the Division of Chemical Sciences, office of the Basic Energy Sciences, U.S. Department of Energy, under Contract DE-AC03-76SF00098.

REFERENCES

1. Poutsma, M., Elek, L. F., Ibarbia, P. A., Risch, A. P., and Rabo, J. A., *J. Catal.* **52,** 157 (1978).
2. Ichikawa, M., *Shokubai* **21,** 253 (1979).
3. Ryndin, Yu. A., Hicks, R. F., Bell, A. T., and Yermakov, Yu. I., *J. Catal.* **70,** 287 (1981).
4. Fajula, F., Anthony, R. G., and Lunsford, J. H., *J. Catal.* **73,** 237 (1982).
5. Vannice, M. A., *J. Catal.* **40,** 129 (1975).
6. Wang, S.-Y., Moon, S. H., and Vannice, M. A., *J. Catal.* **71,** 167 (1981).
7. Poels, E. K., van Broekhoven, E. H., van Barneveld, W. A. A., and Ponec, V., *React. Kinet. Catal. Lett.* **18,** 223 (1981).
8. Ponec, V., *Stud. Surf. Sci. Catal.* **11,** 63 (1982).
9. Poels, E. K., Koolstra, R., Geus, J. W., and Ponec, V., *Stud. Surf. Sci. Catal.* **11,** 233 (1982).
10. Driessen, J. M., Poels, E. K., Hindermann, J. P., and Ponec, V., *J. Catal.* **82,** 26 (1983).
11. Kikuzono, Y., Kagami, S., Naito, S., Onishi, T., and Tamaru, K., *Faraday Discuss. Chem. Soc.* **72,** 135 (1982).
12. Mitchell, M. D., and Vannice, M. A., *Ind. Eng. Chem. Fundam.* **23,** 88 (1984).
13. Boudart, M., and McDonald, M. A., submitted for publication.
14. Fleisch, T. H., Hicks, R. F., and Bell, A. T., *J. Catal.*, **87,** 398 (1984).
15. Hicks, R. F., Yen, Q.-J., and Bell, A. T., *J. Catal.*, **89,** 498 (1984).
16. Hicks, R. F., Yen, A.-J., Bell, A. T., and Fleisch, T. F., *J. Appl. Surf. Sci.*, in press.
17. Hicks, R. F., and Bell, A. T., *J. Catal.*, in press.
18. Hicks, R. F., Kellner, C. S., Savatsky, B. J., Hecker, W. C., and Bell, A. T., *J. Catal.* **71,** 216 (1981).
19. Eischens, R. P., Francis, S. A., and Pliskin, W. A., *J. Phys. Chem.* **60,** 194 (1956).
20. Eischens, R. P., and Pliskin, W. A., "Advances in Catalysis," Vol. 10, p. 1. Academic Press, New York, 1958.
21. Palazov, A., Chang, C. C., and Kokes, R. J., *J. Catal.* **36,** 338 (1975).
22. van Hardeveld, R., and Hartog, F., "Advances in Catalysis," Vol. 22, p. 75. Academic Press, New York, 1972.
23. Baddour, R. F., Modell, M., and Goldsmith, R. L., *J. Phys. Chem.* **74,** 1787 (1970).
24. Sheppard, N., and Nguyen, T. T., "Advances in Infrared and Raman Spectroscopy" (R. J. H. Clark and R. E. Hester, Eds.), Vol. 5. Heyden & Sons, London, 1978.
25. Palazov, A., Kadinov, G., Bonev, Ch., and Shopov, D., *J. Catal.* **74,** 44 (1982).
26. Bradshaw, A. M., and Hoffmann, F. M., *Surf. Sci.* **72,** 513 (1978).
27. Hoffmann, F. M., *Surf. Sci. Rep.* **3,** 107 (1983).
28. Ortega, A., Hoffmann, F. M., and Bradshaw, A. M., *Surf. Sci.* **119,** 79 (1982).
29. Clarke, J. K. A., Farren, G., and Rubalcava, H. E., *J. Phys. Chem.* **71,** 2376 (1967).
30. Naccache, C., Primet, M., and Mathieu, M. V., *Adv. Chem. Ser.* **121,** 266 (1973).
31. Figueras, F., Gomez, R., and Primet, M., *Adv. Chem. Ser.* **121,** 480 (1973).
32. Soma-Noto, Y., and Sachtler, W. M. H., *J. Catal.* **32,** 315 (1974).
33. Bradshaw, A. M., and Hoffmann, F. M., *Surf. Sci.* **52,** 449 (1975).
34. Anderson, J. R., "Structure of Metallic Catalysts." Academic Press, New York, 1975.
35. Duprez, D., and Miloudi, A., *Stud. Surf. Sci. Catal.* **11,** 179 (1982).
36. Christmann, K., and Demuth, J. E., *J. Chem. Phys.* **76,** 6308, 6318 (1982).
37. Gates, J. A., and Kesmodel, L. L., *J. Catal.* **83,** 437 (1983).
38. Vannice, M. A., *J. Catal.* **44,** 152 (1976).
39. Kellner, C. S., and Bell, A. T., *J. Catal.* **75,** 251 (1982).